

1 **Engineered toxin-intein antimicrobials can selectively target and**
2 **kill antibiotic-resistant bacteria in mixed populations**

3

4

5

6 Rocío López-Igual^{1a}, Joaquín Bernal-Bayard², Alfonso Rodríguez-Patón³, Jean-Marc Ghigo²
7 and Didier Mazel^{1*}.

8 ¹Unité de Plasticité du Génome Bactérie, Département Génomes et Génétique, Institut
9 Pasteur, UMR3525, CNRS, Paris, France.

10 ²Unité de Génétique des Biofilms, Département Microbiologie, Institut Pasteur, Paris,
11 France.

12 ³Universidad Politécnica de Madrid, Departamento de Inteligencia Artificial, ETSIINF, 28040
13 Madrid, Spain.

14

15

16

17

18 ^aCurrent Adress: Instituto de Bioquímica Vegetal y Fotosíntesis, CSIC and Universidad de
19 Sevilla, Seville, Spain.

20 *Correspondence should be addressed to D.M. (mazel@pasteur.fr)

21 **Targeted killing of pathogenic bacteria without harming beneficial members of host**
22 **microbiota holds promise as a strategy to cure disease, and limit both antimicrobial-**
23 **related dysbiosis and development of antimicrobial resistance. We engineer toxins**
24 **that are split by inteins and deliver them by conjugation into a mixed population of**
25 **bacteria. Our toxin-intein antimicrobial is only activated in bacteria that harbor**
26 **specific transcription factors. We apply our antimicrobial to specifically target and kill**
27 **antibiotic resistant *Vibrio cholerae* in complex populations gathering various bacterial**
28 **species. We found that 100% of antibiotic resistant *V. cholerae* receiving the plasmid**
29 **were killed. Escape mutants were extremely rare (10⁻⁶-10⁻⁸). We demonstrate that**
30 **conjugation and specific killing of targeted bacteria is functional in the microbiota of**
31 **zebrafish and crustacean larvae, which are natural hosts for *Vibrio* spp. Toxins split**
32 **with inteins could form the basis of a range of precision antimicrobials which would**
33 **kill both Gram – and Gram + pathogens.**

34
35

36 With the advent of the antibiotic era, infectious diseases were thought to be under
37 control, but worldwide emergence of antibiotic-resistant bacteria has occurred, owing to the
38 widespread unchecked use of antibiotics. Further, it is now estimated that antibiotic resistant

39 bacteria could be the main cause of death by 2050¹ unless new classes of antimicrobials are
40 developed.

41 Broad spectrum antimicrobials indiscriminately kill bacteria which can result in
42 microbiota dysbiosis and concomitant health sequelae. Moreover, antibiotic that have non-
43 specific targets can select for antibiotic resistance, which is mainly acquired by horizontal
44 gene transfer among bacteria in communities². Alternatives to broad spectrum antibiotics
45 include bacteriocins, which kill a subset of bacterial species or strains, and will not provoke a
46 superinfection³. Other targeted antimicrobials have also been reported, including CRISPR-
47 Cas antimicrobials⁴⁻⁶, phage therapy⁷ and local release of toxins⁸.

48 We set out to design antimicrobials to specifically kill antibiotic-resistant *Vibrio*
49 *cholerae*. To mediate bacterial killing we chose the toxin component of type II bacterial toxin-
50 antitoxin (TA) systems, which are involved in stabilization of plasmids, prophages and
51 superintegrans⁹. Type II toxin and antitoxins are proteins⁹. The toxin targets conserved
52 bacterial cellular functions which reduces the potential for development of resistance. Each
53 antitoxin is highly specific for the cognate toxin, and nonspecific toxin-antitoxin interactions
54 are counterselected¹⁰. Our antimicrobial design relies on the regulation of type II TA
55 transcription by highly specific transcription factors (TF). This means that activation of the
56 toxin, and concomitant killing, of individual members of mixed bacterial populations is
57 feasible if a targeted bacterial species expresses the Type II toxin-regulating transcription

58 factor. We validated our approach by showing that we could selectively kill antibiotic-
59 resistant *V. cholerae* present in mixed populations.

60 *V. cholerae* causes between 21 000 and 143 000 deaths from cholera per year¹¹.

61 The most recent cholera pandemics involved the O1 and O139 serogroups. Virulence in *V.*
62 *cholerae* is coordinated by the master transcriptional activator ToxR, which regulates the
63 ToxR regulon¹², which includes the cholera toxin genes. Cholera epidemics are associated
64 with antibiotic resistance owing to resistance genes present on an integrative and
65 conjugative element (ICE) named SXT (from sulfamethoxazole and trimethoprim resistance).
66 SXT can carry genes that confer resistance to sulfamethoxazole (*sul2*), trimethoprim (*dfrA1*
67 and *dfr18*), streptomycin (*strB*), chloramphenicol (*floR*) and tetracycline (*tetA*) and was first
68 described in *V. cholerae* serogroup O139¹³. SXT also encodes functions promoting its
69 excision, dissemination by conjugation, and integration, as well as the transcription factors
70 that control expression of these functions¹³.

71 Our previous experience with type II toxins^{14,15} taught us that basal expression of a
72 full-length toxin gene from P_{BAD} is sufficient to kill the *E. coli* host. To avoid this, we
73 designed a genetic module containing a toxin split by an intein, and in our module the split
74 toxin-intein can only be activated by ToxR. Inteins are protein sequences embedded into a
75 host protein (extein) from which they are autocatalytically excised in a process called protein
76 splicing. During protein splicing the intein ligates the extein extremities and allows the

77 reconstitution of the mature protein. In nature, a few examples of split inteins also exist
78 allowing the assembly of a single protein from two genes¹⁶. We split the type II toxin gene
79 *ccdB* (Plasmid pToxInt, Supplementary Fig. 1) into two parts, each of which is associated
80 with half of a split intein. Split inteins have been used in several biotechnological tools¹⁷ and
81 enable control of toxic protein functions *in vivo*¹⁸. We used the split intein DnaE, which is
82 present in the *dnaE* gene of *Nostoc punctiforme*. DnaE is well characterized and has a high
83 rate of trans-splicing¹⁹. Using inteins enables strict control of toxin production, and avoids
84 toxicity due to basal expression^{14,15} (Supplementary Fig. 1).

85 First, we cloned full –length gyrase inhibiting toxin CcdB from *Vibrio fischeri*¹⁵ into a
86 plasmid (pTOX Supplementary Table 1) and transformed the toxin construct into a *E. coli*
87 XL2 blue (Supplementary Table 1) that constitutively expresses a genomic copy of the
88 cognate antitoxin (data not shown). We showed that *ccdB* was bactericidal (Supplementary
89 Fig. 2) and that the intein-mediated splitting strategy led to more stable retention of the toxin-
90 harboring plasmid under repression conditions compared with a construct harboring a whole
91 *ccdB* toxin gene (Supplementary Fig. 1). We also evaluated whether three other type II
92 toxins belonging to different toxin families (ParE2, HigB2 and RelE4¹⁴) could tolerate a
93 splitting and stay functional, We selected intein insertion points by inspection of 3D structure
94 predictions for toxins made in Phyre2²⁰, a tool for modeling protein structure (Supplementary
95 Fig. 3a). Each toxin was divided into N- and C-terminal portions (Supplementary Fig. 3b)

96 which were fused in-frame to the N- or C-parts of the split intein *dnaE* gene (102 and 36
97 amino acids long), respectively. N- and C-terminal toxin-intein fusions were cloned in
98 separate, compatible plasmids (N or C plasmids, respectively Supplementary Table 1) and
99 were under the control of different promoters (Fig. 1a). We validated reconstitution of the
100 active toxin by intein protein splicing in *E. coli* (Supplementary Fig. 4). For all five tested split
101 toxins, we found that under inducing conditions bacteria containing N and C plasmids died,
102 whereas bacteria with either the N or the C plasmid survived. N and C toxin-intein complex
103 toxicity was tested using mutations known to prevent splicing. When splicing didn't occur,
104 reconstitution of the toxin did not take place, and bacteria survived (Supplementary Fig. 4).

105 Next we chose the gyrase poison CcdB, which is likely the most extensively
106 characterized type II toxin, to design a toxin-intein antimicrobial specific for pathogenic *V.*
107 *cholerae*. In *V. cholerae* one of the ToxRS-regulated genes encodes a membrane porin,
108 OmpU²¹. We cloned the N fusion of CcdB-intein downstream of the *ompU* promoter
109 (regulated by ToxRS), and the C fusion under P_{BAD} in the same plasmid (pU-BAD,
110 Supplementary Fig. 5a). The functionality of pU-BAD was tested in an *E. coli* DH5α strain
111 expressing the *V. cholerae* *toxRS* operon from a second plasmid (pRS, Supplementary Fig.
112 5a). Upon arabinose-mediated induction of *toxRS* expression, only bacteria containing both
113 pU-BAD and pRS plasmids died (Supplementary Fig. 5b). We replicated cell killing in
114 MG1655 (data not shown). We then tested pU-BAD activity in pathogenic *V. cholerae* strains

115 O1 and O139 (Supplementary Fig. 6a). We observed constitutive expression of the N-fusion
116 due to the presence of chromosomal *toxRS*. However, toxicity due to basal expression from
117 P_{BAD} (Supplementary Fig. 6a) led to pU-BAD plasmid instability in *V. cholerae*. A *V. cholerae*
118 mutant lacking *toxRS* (Δ *toxRS*) displayed normal growth and pU-BAD stability in the
119 presence of arabinose (Supplementary Fig. 6a). This suggested that P_{ompU} could be used to
120 regulate CcdB-intein fusion expression for targeted killing of *V. cholerae*.

121 In order to develop a conjugative CcdB-intein-based antimicrobial to specifically kill
122 pathogenic *V. cholerae* in microbial communities, we cloned a split-toxin-intein operon under
123 the control of *ompU* promoter in a plasmid, and added an origin of transfer (*oriT*) to render it
124 conjugative (plasmid pPW, Supplementary Fig. 6b, Supplementary Table 1). Conjugation is
125 carried out from donor strain *E. coli* β 3914, an MG1655 Δ *dapA* which contains the RP4
126 conjugative machinery integrated into its chromosome. pPW was introduced by conjugation
127 into *V. cholerae* strains O1, O139 and an O1- Δ *toxRS* mutant (Supplementary Fig. 6b), but
128 only the Δ *toxRS* strain was able to grow after transfer of the pPW plasmid, demonstrating
129 that it kills only *Vibrio* expressing ToxR.

130 We next tested whether pPW could kill specific strains in a mixed bacterial population
131 (Fig. 1b). Different recipient bacteria in this population could be distinguished in the
132 presence of X-gal: *V. cholerae* O139 (blue) and *E. coli* DH5 α (white) (Fig. 1c). We
133 conjugated pPW and two control plasmids (non-toxic N fusion containing pN_{ctrl} plasmid, and

134 the pTox_{ctrl} plasmid, which carries the P_{BAD}-regulated toxin-intein operon) into this mixture.
135 After conjugation of pPW from *E. coli* β3914 and selection for transconjugants, pPW killed *V.*
136 *cholerae* O139 (blue bacteria) and we were only able to detect *E. coli* DH5α transconjugants
137 (white) on media containing XGal. Similarly, after plasmid conjugation into *V. cholerae* O1
138 and *E. coli* strains (MG1655), we only obtained *E. coli* transconjugants (Supplementary Fig.
139 7a).

140 Specific killing by pPW relies on expression of the regulator *toxR*, which is present in
141 all *Vibrio* genera²². However, the ToxR regulon has evolutionarily diverged among the
142 different *Vibrio* species, so we analyzed pPW action in two other *toxRS*-containing *Vibrio*
143 species (Fig. 1d). We found that pPW can kill *Vibrio mimicus* but not *Vibrio vulnificus*, which
144 is more phylogenetically distant from *V. cholerae*, and despite harboring a ToxR ortholog,
145 does not activate *ompU* expression²³. Additionally, we showed that our system is highly
146 specific to ToxR, since conjugation into other γ-proteobacteria, such as *Salmonella*
147 *typhimurium* and *Citrobacter rodentium*, did not result in killing (Supplementary Fig. 7b).

148 Next we evaluated whether a split-intein toxin could kill antibiotic resistant bacteria
149 present in a community. The SXT ICE family in *V. cholerae* includes various antibiotic
150 resistance genes¹³. The SXT chassis encodes several TFs that regulate SXT transmission
151 including the SetR repressor¹³. We designed a module to detect SXT carriage and kill SXT-
152 harboring bacteria by implementing an additional component into our antimicrobial: the *ccdA*

153 gene, which encodes the antitoxin partner of CcdB. *ccdA* was cloned downstream of the
154 SXT PL promoter, which is controlled by the SetR repressor, in a plasmid also containing the
155 *ccdB*-intein operon regulated by the P_{BAD} promoter (pPLA plasmid, Supplementary Fig. 8a,
156 Supplementary Table 1). We tested whether pPLA could kill antibiotic resistant *E. coli* SXT
157 (Supplementary Fig. 8b) and *V. cholerae* O139 (Fig. 2a). Both bacteria contain an SXT
158 element integrated at *prfC*. Only SXT carrying bacteria from both species were killed. All
159 bacteria lacking SXT, including *V. cholerae* O1 and *E. coli* DH5 α , survived (Fig. 3a and
160 Supplementary Fig. 8b). In order to develop a conjugative antimicrobial to kill antibiotic
161 resistant bacteria we added an *oriT* to pPLA to produce pABRW (Supplementary Table 1,
162 Fig. 2). pABRW was tested by conjugation into a mixed population of *E. coli* MG1655 (blue)
163 and *E. coli* SXT (white). Selection for pABRW yielded only *E. coli* MG1655 transconjugants,
164 demonstrating that pABRW specifically kills bacteria containing SXT (Fig. 2b). The same
165 result was obtained after conjugation of pABRW into *V. cholerae* O139 mixed with *V.*
166 *cholerae* O1- Δ *lacZ* (Fig. 2c), confirming that pABRW plasmid specifically kills ABR bacteria
167 in a heterogeneous population.

168 We next combined the pPW and pABRW modules in a single plasmid. We replaced
169 the operator sequence O4 of PL with O1 (see online Methods) to increase SetR repression
170 to yield pFW (Supplementary Table 1, Fig. 3), which efficiently kills *V. cholerae* O139 (Fig.
171 3c). In order to test whether non-replicative-conjugative plasmids (which would not spread

172 toxin-intein fusions and/or antibiotic resistant genes) could harbor our killing module, we
173 changed the pSC101 replication origin to a *pir*-dependent R6K origin (Supplementary Fig.
174 9). R6K origin can be activated in a host expressing an ectopic *pir* gene in the chromosome.
175 After conjugation of pPW-R6K and pFW-R6K into bacteria that lack the *pir* gene, CFU/ml
176 were reduced by 60% compared with controls (Supplementary Fig. 9b). This suggests that
177 even if the plasmid cannot actively replicate once transferred in the targeted bacteria,
178 expression of the toxin is sufficient to kill these bacteria, while the use of such R6K
179 derivatives is limiting the risk of unnecessary propagation of the killing plasmid.

180 We moved onto evaluate whether our split-intein toxin could target specific bacteria
181 in natural microbiomes. We tested killing of *V. cholerae* O139 in three niches, each of which
182 is a natural habitat for this pathogen²⁴: water, tropical zebrafish and a crustacean. We first
183 tested the versatility of *E. coli* β 3914 which is auxotrophic for the diaminopimelic acid (DAP)
184 for delivering conjugative plasmid pNctrl, in absence of DAP and found no difference in
185 conjugation rates (Supplementary Table 2). Although conjugation efficiency decreases 300
186 fold in water, *V. cholerae* transconjugants were obtained with the control plasmid pN_{ctrl}
187 (Supplementary Table 2), while using pFW, no transconjugants were detected (data not
188 shown). These results indicate that in these conditions too when receiving the pFW, *V.*
189 *cholerae* was killed. These preliminary data suggest that our method using pFW might hold
190 potential in bioremediation of *Vibrio*-contaminated water.

191 We also tested pNctrl and pFW using a zebrafish infection model²⁵ (Supplementary
192 Fig. 10a). Analysis of the microbiota composition using 16S rRNA analysis on 4 days post
193 fertilization zebrafish larvae detected less than 30 different bacterial species, mostly aerobic
194 including several *Aeromonads*, *Pseudomonads* and *Stenotrophimonads* (JBB and JMG,
195 unpublished). First we tested localization of both *E. coli* and *V. cholerae*, in the gut of
196 zebrafish larvae. We infected four-day-post-fertilization zebrafish larvae with fluorescently
197 tagged *V. cholerae* O1-GFP and *E. coli*-RFP. Fluorescence microscopy revealed co-
198 localization of both *V. cholerae* O1-GFP and *E. coli*-RFP in the digestive tract
199 (Supplementary Fig. 10a). We then tested specific killing in larvae infected with *V. cholerae*
200 O139 (Fig. 4a, Supplementary Fig. 11b,c). The only *V. cholerae* O139 transconjugants
201 obtained were from conjugation with pN_{ctrl} plasmid. No *V. cholerae* O139 transconjugants
202 were obtained using pFW. Therefore, pFW kills *V. cholerae* O139 in zebrafish larvae (Fig. 4a
203 and Supplementary Fig. 11b). We assessed dysbiosis using observation after plating on
204 different media and didn't find any macroscopic change (Supplementary Fig. 11a). We also
205 used a mixture of 1:1 *V. cholerae* O1 and O139 for larval infection and then infected with *E.*
206 *coli* β3914 (pNctrl) or β3914 (pFW). We detected pN_{ctrl} transconjugants in both O1 and O139
207 serogroups, but O1 transconjugants only were obtained after conjugation with pFW (Fig. 4a
208 and Supplementary Fig. 11c). Therefore pFW specifically killed the O139 serogroup.

209 We also tested pFW in the crustacean *Artemia salina* model which is used for fish
210 feeding and commonly found to carry various *Vibrio* species²⁶ (Fig. 4b and Supplementary
211 Figs. 10b, 12). We detected co-localization of *V. cholerae* O1-GFP and *E. coli*-RFP in the
212 gut of *A. salina* (Supplementary Fig. 10b) and conjugation with pFW plasmid did not provoke
213 visible change in the *A. salina* microbiota, after sampling of the aerobic species on plates
214 (data not shown). Transconjugants of *V. cholerae* O139 were only detected after
215 conjugation with pN_{ctrl}, but not with pFW, showing that pFW kills *V. cholerae* O139 in *A.*
216 *salina* larvae (Fig. 4b and Supplementary Fig. 12a). We also infected *A. salina* with a 1:1 mix
217 of *V. cholerae* O1 and O139 and detected pN_{ctrl} transconjugants in O1 and O139
218 serogroups, but only detected O1 pFW transconjugants (Fig. 4b and Supplementary Fig.
219 12b).

220 Our split toxin-intein method can be applied to specifically kill selected bacteria
221 subtypes. We anticipate that our system could be fine-tuned to trigger toxin activation in
222 response to various environmental cues²⁷ including temperature, salt or pH by adding a
223 conditional protein splicing intein²⁸. Inteins are functional in eukaryotic cells²⁹, so toxin-intein
224 combinations might also be developed for targeted killing of tumor cells. The specificity of
225 our system requires identification of a species-specific transcriptional regulator, and such
226 TFs are widespread in pathogenic and antibiotic-resistant bacterial pathogens³⁰⁻³¹. The
227 Achilles' heel of precision antimicrobials is delivery into complex communities. Antimicrobials

228 delivered by conjugation e.g. RNA-guided nucleases⁵ have reduced targeted bacterial
229 populations by 2- to 3-log even with a ratio of donor:recipient bacteria of 340:1⁵. In our
230 experiments, using 1:1 ratios were detected a decrease in targeted bacteria (*V. cholerae*) of
231 10%, which is equivalent to the conjugation rate. We were able to kill \approx 90-95% of the ABR
232 *E. coli* after the conjugation of pABRW by increasing ratios of donor to recipient to 10:1
233 (Supplementary Fig. 13). Phage delivery might be useful⁵, but phage have other
234 disadvantages³², including narrow host range and rapid emergence of phage resistance.
235 One advantage of our system compared with others^{4,5,33} is that escape mutants are less
236 frequent (below 10^{-6} - 10^{-8} ; Supplementary Table 3). Analysis of escape clones
237 (Supplementary Table 4), when targeting ABR bacteria revealed that between 63 and 90%
238 of these clones had lost the SXT element, and were not ABR (Supplementary Table 5). One
239 of the reasons for the lower chance of escape might be that toxin resistance has not been
240 observed. A different synthetic kill switch based on TA systems was also stable due to
241 minimal escape rates *in vivo*³⁴. The dual regulatory system in the Final Weapon (Fig. 3a)
242 functions as an AND-logic gate, increasing effectiveness in the control of toxin production,
243 which only happens when both inputs (pathogenicity and ABR) are present. If delivery of
244 mobilizable antimicrobials can be optimized, appearance of resistant bacteria would be rare.
245

246

247 **REFERENCES**

- 248 1. World Health Organization. The evolving threat of antimicrobial resistance: Options for
249 action. *WHO Publ.* 1–119 (2014).
- 250 2. Davies, J. & Davies, D. Origins and evolution of antibiotic resistance. *Microbiol. Mol.*
251 *Biol. Rev.* **74**, 417–433 (2010).
- 252 3. Chikindas, M. L., Weeks, R., Drider, D., Chistyakov, V. A. & Dicks, L. M. Functions
253 and emerging applications of bacteriocins. *Current Opinion in Biotechnology* **49**, 23–
254 28 (2018).
- 255 4. Bikard, D. *et al.* Exploiting CRISPR-Cas nucleases to produce sequence-specific
256 antimicrobials. *Nat. Biotechnol.* **32**, 1146–50 (2014).
- 257 5. Citorik, R. J., Mimee, M. & Lu, T. K. Sequence-specific antimicrobials using efficiently
258 delivered RNA-guided nucleases. *Nat. Biotechnol.* **32**, 1141–1145 (2014).
- 259 6. Rodriguez-Pagan, I., Novick, R. P., Ross, H. F., Jiang, D. & Ram, G. Conversion of
260 staphylococcal pathogenicity islands to CRISPR-carrying antibacterial agents that
261 cure infections in mice. *Nat. Biotechnol.* (2018). doi:10.1038/nbt.4203
- 262 7. Lin, D. M., Koskella, B. & Lin, H. C. Phage therapy: An alternative to antibiotics in the
263 age of multi-drug resistance. *World J. Gastrointest. Pharmacol. Ther.* **8**, 162 (2017).
- 264 8. Jayaraman, P., Holowko, M. B., Yeoh, J. W., Lim, S. & Poh, C. L. Repurposing a Two-

- 265 Component System-Based Biosensor for the Killing of *Vibrio cholerae*. *ACS Synth.*
266 *Biol.* **6**, 1403–1415 (2017).
- 267 9. Lobato-Márquez, D. *et al.* Toxin-antitoxins and bacterial virulence. *FEMS Microbiol.*
268 *Rev.* **40**, 592–609 (2016).
- 269 10. Goeders, N. & Van Melderen, L. Toxin-antitoxin systems as multilevel interaction
270 systems. *Toxins* **6**, 304–324 (2013).
- 271 11. Ali, M., Nelson, A. R., Lopez, A. L. & Sack, D. A. Updated global burden of cholera in
272 endemic countries. *PLoS Negl. Trop. Dis.* **9**, 1–13 (2015).
- 273 12. Childers, B. M. & Klose, K. E. Regulation of virulence in *Vibrio cholerae*: the ToxR
274 regulon. *Future Microbiol.* **2**, 335–344 (2007).
- 275 13. Beaber, J. W., Hochhut, B. & Waldor, M. K. SOS response promotes horizontal
276 dissemination of antibiotic resistance genes. *Nature* **427**, 72–74 (2004).
- 277 14. Iqbal, N., Guérout, A. M., Krin, E., Le Roux, F. & Mazel, D. Comprehensive functional
278 analysis of the 18 *Vibrio cholerae* N16961 toxin-antitoxin systems substantiates their
279 role in stabilizing the superintegron. *J. Bacteriol.* **197**, 2150–2159 (2015).
- 280 15. Guérout, A. M. *et al.* Characterization of the phd-doc and ccd toxin-antitoxin cassettes
281 from *Vibrio* superintegrons. *J. Bacteriol.* **195**, 2270–2283 (2013).
- 282 16. Topilina, N. I. & Mills, K. V. Recent advances in in vivo applications of intein-mediated
283 protein splicing. *Mob. DNA* **5**, 5 (2014).

- 284 17. Li, Y. Split-inteins and their bioapplications. *Biotechnology Letters* **37**, 2121–2137
285 (2015).
- 286 18. Alford, S. C., O'Sullivan, C., Obst, J., Christie, J. & Howard, P. L. Conditional protein
287 splicing of [small alpha]-sarcin in live cells. *Mol. Biosyst.* **10**, 831–837 (2014).
- 288 19. Zettler, J., Schütz, V. & Mootz, H. D. The naturally split Npu DnaE intein exhibits an
289 extraordinarily high rate in the protein trans-splicing reaction. *FEBS Lett.* **583**, 909–
290 914 (2009).
- 291 20. Kelley, L. A., Mezulis, S., Yates, C. M., Wass, M. N. & Sternberg, M. J. E. The Phyre2
292 web portal for protein modeling, prediction and analysis. *Nat. Protoc.* **10**, 845–858
293 (2015).
- 294 21. Crawford, J. A., Kaper, J. B. & DiRita, V. J. Analysis of ToxR-dependent transcription
295 activation of *ompU*, the gene encoding a major envelope protein in *Vibrio cholerae*.
296 *Mol. Microbiol.* **29**, 235–246 (1998).
- 297 22. Osorio, C. R. & Klose, K. E. A region of the transmembrane regulatory protein ToxR
298 that tethers the transcriptional activation domain to the cytoplasmic membrane
299 displays wide divergence among vibrio species. *J. Bacteriol.* **182**, 526–528 (2000).
- 300 23. Lee, S. E. *et al.* *Vibrio vulnificus* has the transmembrane transcription activator ToxRS
301 stimulating the expression of the hemolysin gene *vvhA*. *J. Bacteriol.* **182**, 3405–3415
302 (2000).

- 303 24. Vezzulli, L., Pruzzo, C., Huq, A. & Colwell, R. R. Environmental reservoirs of *Vibrio*
304 *cholerae* and their role in cholera. *Environmental Microbiology Reports* **2**, 27–33
305 (2010).
- 306 25. Runft, D. L. *et al.* Zebrafish as a natural host model for *Vibrio cholerae* colonization
307 and transmission. *Appl. Environ. Microbiol.* **80**, 1710–1717 (2014).
- 308 26. Austin, B., Austin, D., Sutherland, R., Thompson, F. & Swings, J. Pathogenicity of
309 vibrios to rainbow trout (*Oncorhynchus mykiss*, Walbaum) and *Artemia* nauplii.
310 *Environ. Microbiol.* **7**, 1488–1495 (2005).
- 311 27. Lennon, C. W. & Belfort, M. Inteins. *Current Biology* **27**, R204–R206 (2017).
- 312 28. Callahan, B. P., Topilina, N. I., Stanger, M. J., Van Roey, P. & Belfort, M. Structure of
313 catalytically competent intein caught in a redox trap with functional and evolutionary
314 implications. *Nat. Struct. Mol. Biol.* (2011). doi:10.1038/nsmb.2041
- 315 29. Zhu, F. X. *et al.* Inter-chain disulfide bond improved protein trans-splicing increases
316 plasma coagulation activity in C57BL/6 mice following portal vein FVIII gene delivery
317 by dual vectors. *Sci. China Life Sci.* **56**, 262–267 (2013).
- 318 30. Hacker, J. & Kaper, J. B. PATHOGENICITY ISLANDS AND THE EVOLUTION OF
319 MICROBES. *Annu. Rev. Microbiol* **54**, 641–79 (2000).
- 320 31. Main-Hester, K. L., Colpitts, K. M., Thomas, G. A., Fang, F. C. & Libby, S. J.
321 Coordinate regulation of *Salmonella* pathogenicity island 1 (SPI1) and SPI4 in

- 322 *Salmonella enterica* serovar typhimurium. *Infect. Immun.* (2008).
- 323 doi:10.1128/IAI.01224-07
- 324 32. Loc-Carrillo, C. & Abedon, S. Pros and cons of phage therapy. *Bacteriophage* **1**, 111–
- 325 114 (2011).
- 326 33. Yosef, I., Manor, M., Kiro, R. & Qimron, U. Temperate and lytic bacteriophages
- 327 programmed to sensitize and kill antibiotic-resistant bacteria. *Proc. Natl. Acad. Sci.*
- 328 **112**, 7267–7272 (2015).
- 329 34. Stirling, F. *et al.* Rational Design of Evolutionarily Stable Microbial Kill Switches. *Mol.*
- 330 *Cell* **68**, 686–696 (2017).
- 331
- 332

333

334 **ACKNOWLEDGMENTS**

335 We would like to thank E. Krin and M. Gugger for providing chromosome DNA for *V.*
336 *cholerae* and *V. fischeri*, and *N. punctiforme* cells, respectively and V. Burrus for *V. cholerae*
337 O139. We thank G. Cambray and Z. Baharoglu for *V. cholerae*-GFP strain and RFP-
338 containing plasmid, respectively. We thank S. Jin for her technical help. We thank also P.
339 Escoll for assistance with microscopy, Valerie Briolat for providing us with the zebrafish and
340 Artemias, A. Gomez-Losada for his help with the statistics treatment, and S. Aguilar-Pierlé
341 for helpful reading of the manuscript. We thank F. de la Cruz for his invaluable comments
342 along the development of this work. This work was supported by the Institut Pasteur (D.M.
343 and J.-M.G. Units), the Centre National de la Recherche Scientifique (CNRS-UMR 3525)
344 (D.M.), PLASWIRES 612146/FP7- FET-Proactive (D.M., A.R.-P Lab, R.L.-I. salary), the
345 French Government's Investissement d'Avenir program, Laboratoire d'Excellence
346 "Integrative Biology of Emerging Infectious Diseases" (grant n°ANR-10-LABX-62-IBEID to D.
347 M. and J.-M.G. Units), Spanish project TIN2016-81079-R (AEI/FEDER, EU) and Comunidad
348 de Madrid (cofound with FES and FEDER, EU) B2017/BMD-3691 project ingeMICS-CM
349 (A.R.-P), the Fondation pour la Recherche Médicale (Grant No. DBF20160635736 to D.M.
350 and DEQ20140329508 to J.-M.G.). J.B.-B. was the recipient of a long-term post-doctoral
351 fellowship from the Federation of European Biochemical Societies (FEBS).

352

353 **AUTHOR CONTRIBUTIONS**

354 D.M. and R.L.-I designed the experiments. J.B.-B and R.L.-I designed and performed the *in*
355 *vivo* experiments. J.B.-B. performed the microscopy experiments and statistic analysis.

356 D.M., R.L.-I and A.R.-P participated in the conception of the project. R.L.-I and D.M.

357 prepared the manuscript and wrote the article with large participation of J.B.-B, J.-M.G. and

358 A.R.-P.

359

360 **COMPETING FINANCIAL INTERESTS**

361 The authors declare no competing financial interests.

362

363 **DATA AVAILABILITY STATEMENT**

364 The data, plasmids and strains generated for this study, that support our findings are

365 available upon request to the corresponding author.

366

367 **Figure Legends:**

368 **Figure 1. Specific killing of pathogenic *V. cholerae* in mixed population of**
369 **bacteria mediated by toxin-intein strategy.** (a) Schematic representation of the
370 active toxin production from plasmids encoding split toxin (red) combined with split
371 intein (blue) inside a bacterium. The first half of the toxin is fused with N-terminal split
372 intein gene (N plasmid) under the control of P_{BAD} promoter and the second half of the
373 toxin is fused with the C-terminal intein gene (C plasmid) and it is controlled by P_{LAC}.
374 Expression of these fusions is activated by the addition of arabinose and IPTG,
375 respectively. Recognition of the protein fusions takes place by the intein module,
376 which carry out the splicing process, which lead to toxin reconstitution, provoking cell
377 death. (b) Mode of action of the genetic weapon spreading through conjugation in
378 mixed population of bacteria and killing of targeted harmful bacteria. (c) Mixed
379 population of *V. cholerae* O139 (blue) and *E. coli* DH5 α (white) as recipients for
380 conjugation using β 3914 as donor strain containing pN_{ctrl}, pTox_{ctrl} or pPW plasmids.
381 The *ompU* promoter activated specifically by ToxRS from *V. cholerae* is represented
382 by a circled (+) pink-symbol. Transconjugants were selected in MH + Spectinomycin
383 (Sp), X-gal for color development and arabinose for induction of P_{BAD}. (d)
384 Conjugation of pN_{ctrl}, pTox_{ctrl} and pPW plasmid using β 3914 as donor strain in *Vibrio*
385 *mimicus* and *Vibrio vulnificus*. Transconjugants were selected in MH media + Sp and
386 arabinose for induction of P_{BAD}. Pictures are representative of three independent
387 experiments.

388

389

390 **Figure 2. Specific killing of antibiotic resistant bacteria (containing SXT).** (a)

391 pPLA plasmid that contains CcdB-intein fusion operon under P_{BAD} control expression

392 and *ccdA* antitoxin under PL promoter (symbolized by an orange circled -) which is
393 repressed by SetR. Growth test of *V. cholerae* O1 or O139 containing pPLA plasmid
394 in MH media + Sp and supplemented with glucose (GLU) or arabinose (ARA). (b)
395 Mixed population of *E. coli* MG1655 (blue) and *E. coli* SXT (white) as recipients for
396 conjugation using β 3914 as donor strain containing pN_{ctrl}, pTox_{ctrl} or pABRW
397 plasmids. Transconjugants were selected on MH + Sp, X-gal for species
398 identification and arabinose for induction of P_{BAD}. (c) Mixed population of *V. cholerae*
399 O139-SXT (blue) and *V. cholerae* O1 (white) as recipients for conjugation using
400 β 3914 as donor strain containing pN_{ctrl}, pTox_{ctrl} or pABRW plasmids as described in
401 b). Pictures are representative of three independent experiments.

402

403

404 **Figure 3. Design, tuning and assay of the final weapon pFW, obtained by**
405 **putting together the pathogenicity and antibiotic resistance (ABR) modules in**
406 **a single conjugative vector.** (a) Schematic representation of the specific killing of
407 *V. cholerae* O139 after pFW conjugation (left). Schematic display of the
408 corresponding AND-logic gate (right). (b) Conjugation from β 3914 of either pN_{ctrl} or
409 pFW, of *V. cholerae* serogroup O139 (blue) and O1 (white) as recipient mixed
410 population. Transconjugants were selected on MH + Sp (plasmid marker). pFW
411 plasmid was obtained after change in RBS sequence of *ompU* promoter to increase
412 translation of toxin-intein fusion and substitution of the O4 operator sequence by O1
413 operator sequence (see online methods) to increase SetR binding affinity to the PL
414 promoter, and consequently increase repression. Only *V. cholerae* serogroup O1
415 that is devoid of SXT in its genome was detected after pFW conjugation,
416 demonstrating the specific killing of serogroup O139, which contain both
417 chromosomally encoded ToxR and SetR the chosen indicators of pathogenicity and

418 antibiotic resistance, respectively. Pictures are representative from three
419 independent experiments.

420

421

422 **Figure 4. Specific killing of pathogenic and ABR *V. cholerae* O139 in the**
423 **zebrafish larvae and *Artemia salina* nauplii models.** (a) Four-day-postfertilization
424 zebrafish larvae were exposed to water containing 10^4 CFU/ml *V. cholerae* O139 or
425 a mixed population containing 10^5 CFU/ml *V. cholerae* O139 + *V. cholerae* O1, and
426 then infected (see methods) with 10^7 (O139) or 10^6 (mix *Vibrio*) CFU/ml of β 3914 as
427 donor strain of either pN_{ctrl} or pFW plasmids. Five larvae were fished and mashed to
428 analyze its microbiota. Transconjugants were selected in MH media with Sp and X-
429 gal. Transconjugants were only detected after conjugation with pN_{ctrl} plasmid for
430 O139 and not after pFW conjugation as expected from the specific killing. Confirming
431 pFW specificity, pFW transconjugants were detected for *V. cholerae* O1, which should
432 not be killed by this plasmid. Data for O139 represent transconjugants obtained from
433 15 larvae fished in three independent experiments (n=3, mean \pm s.d), and data from
434 the mix of *Vibrio* represent transconjugants obtained from 10 larvae in two
435 independent experiments (n=2, mean \pm s.d). (b) *Artemia salina* stage nauplii were
436 infected with 10^7 CFU/ml *V. cholerae* O139 or a mix of 10^7 CFU/ml *V. cholerae* O139
437 + *V. cholerae* O1 (see methods). Then exposed to 10^7 CFU/ml β 3914 as donor strain
438 of either pN_{ctrl} or pFW plasmids. Transconjugants were selected in MH media with
439 Sp and X-gal. As in zebrafish, transconjugants were only detected after conjugation
440 with pN_{ctrl} plasmid for O139 and not after pFW conjugation. As expected, *V.*
441 *cholerae* O1 pFW transconjugants were also detected in this in vivo model. Data
442 numbers were calculated from four independent experiments (n=4, mean \pm s.d).

443

1 ONLINE METHODS

2

3 **Strains and culture conditions.**

4 Unless otherwise noted, bacterial cultures were grown at 37°C with Luria-Bertani (LB)
5 medium (Lennox) or Mueller-Hinton (MH) solid media supplemented when appropriate,
6 with the following antibiotics: 50 µg/ml kanamycin (Kan), 50 µg/ml chloramphenicol
7 (Cm), 100 µg/ml carbenicillin (Carb), 50 or 100 µg/ml spectinomycin (Sp) for *E. coli* and
8 100 µg/ml Sp for *Vibrio cholerae*. Selection of transconjugants was carried using 100
9 µg/ml Sp in all cases, except for *V. mimicus* and *V. vulnificus* where we used 50 µg/ml
10 Sp. Bacterial strains used in this study are listed in Supplementary Table 1. Other
11 molecules were added to the media with the following concentrations: 40 µg/ml 5-
12 bromo-4-chloro-3-indolyl-beta-D-galactopyranoside (Xgal), 0.3 mM Diaminopimelic acid
13 (DAP), 1% glucose and 0,2% arabinose.

14

15 **Plasmid construction.**

16 Plasmids are listed in Supplementary Table 1 and primers in Supplementary Table 6.
17 All plasmid sequences were verified through sequencing.
18 To generate the N and C plasmids for each toxin-intein fusion, the N- and C-terminal
19 toxin regions were amplified with primers F-toxin-EcoRI/R-toxin-intein and F-toxin-
20 intein/R-toxin-Xbal, respectively. N-and C-terminal intein regions were amplified with
21 primers F-intein-toxin/R-intein-Xbal and F-intein-EcoRI/R-intein-toxin, respectively. As
22 DNA templates for toxins we used chromosomal DNA from *V. cholerae* in all cases and
23 *V. fischeri* for *ccdB*. Intein amplification was done with chromosomal DNA from the
24 cyanobacteria *Nostoc punctiforme*. PCR products of N- and C-terminal regions were
25 fused by Gibson assembly³⁵. Each toxin-intein fusion was then digested with
26 EcoRI/Xbal (Thermo Fisher) and then cloned in EcoRI/Xbal digested pBAD43³⁶ and
27 pSU38³⁷ (or pSU18) plasmids, respectively (Supplementary Table 1). To generate the

28 mutated version of N-terminal plasmid (n*) whole plasmids were amplified using
29 primers F-Int-tox-mut/R-int-tox-mut.

30 To assemble the pU-BAD plasmid (Supplementary Fig. 5) we first cloned the C-
31 terminal CcdB-Npu fusion into a pBAD18 plasmid (EcoRI-XbaI). An *ompU* promoter
32 was inserted upstream the N-terminal ccdB/Npu fusion in N plasmid by PCR. The
33 *ompU* promoter region was amplified using F-PompU-1/R-PompU-dB (size=352 bp).
34 This promoter was chosen based on previous work²¹ that showed its high induction in
35 the presence of ToxR. A region containing the pSC101 origin was amplified using R-
36 BAD43-BAD18/F-4126 primers and the N-terminal CcdB-Npu plasmid as template. A
37 second region containing the N-terminal fusion was amplified using 4217/R-BAD43-
38 BAD18 primers and N-terminal plasmids also as templates. Other regions containing
39 the C-terminal fusion and Kan resistance gene were amplified using R-BAD18-
40 BAD43/F-BAD18-BAD43 primers and the C-terminal CcdB-Npu pBAD18 plasmid as
41 template. PCR products were then fused by Gibson assembly³⁵ producing the pU-BAD
42 plasmid.

43 To generate the pRS plasmid, (Supplementary Fig. 5) the *toxRS* operon from *V.*
44 *cholerae* O1 was amplified using F-toxR-SacI/R-toxS-XbaI primers, digested with SacI
45 and XbaI and ligated with SacI-XbaI digested plasmid pBAD30. The native RBS
46 sequence of *toxR* was kept.

47 To assemble the toxin-intein N and C-terminal fusions as an operon (pToxInt plasmid),
48 N- and C-fusions were amplified using F-CcdB-EcoRI/R-Int-N-Int-C and F-Int-C-Int-
49 N/R-Int-XbaI primers and then ligated by Gibson assembly³⁵, digested with EcoRI/XbaI
50 and cloned into a pBAD43-EcoRI/XbaI digested plasmid. The fusion contains the
51 following sequence: 5' TGATAAAGGAGGTAACATATG 3' between the N and C genes.
52 This sequence contains the RBS sequence necessary for translation of the C-terminal
53 fusion. The pTox plasmid was created by amplification of the *ccdB* toxin gene from *V.*
54 *fischeri* DNA with F-CcdB-EcoRI/R-CcdB-XbaI primers, EcoRI/XbaI digestion and
55 ligation into a pBAD43-EcoRI/XbaI digested plasmid. *E. coli* XL2blue strain that

56 contains F' plasmid integrated in the chromosome (containing the *ccdB/ccdA* TA
57 system and conferring resistance to CcdB), was used to transform with this ligation in
58 order to obtain positive clones.

59 To assemble the pPW genetic weapon, the *ompU* promoter was amplified as
60 previously described and ligated by Gibson assembly³⁵ with the product of pToxInt
61 plasmid PCR using F-dB-PompU/R-BAD-PU1 primers.

62 The pPLA plasmid was constructed first by amplifying by PCR the PL promoter³⁸ using
63 DNA from *V. cholerae* O139 and F-PL-plasmid/R-PL-*ccdA* as primers. Then, the *ccdA*
64 antitoxin gene was amplified using the F-*ccdA*-PL/R-*ccdA*-plasmid primers and *V.*
65 *fischeri* DNA. Finally, the pTox-Int plasmid was also amplified using F-plasmid-dA/R-
66 plasmid-PL primers. Ligation by Gibson assembly³⁵ of the three PCR products resulted
67 in the pPLA plasmid.

68 Mobilizable genetic weapons were created by amplifying the origin of transfer *oriT* RP4
69 using F-pSW23-BAD/R-oriT-BAD43 primers and the plasmid pSW23T³⁹ as template.
70 Then, the *oriT* PCR product was ligated through Gibson assembly³⁵ with the amplified
71 plasmid using F-BAD-pSW/R-BAD43-oriT primers and the weapon or control plasmids
72 as template.

73 To assemble the Final Weapon we the plasmid pFW (Figure 3) as follow. The *ompU*
74 promoter-1 was ligated into the pABRW plasmid as previously described for the pU-
75 BAD construction. In order to fine-tune the RBS of *ompU* in this plasmid as well as the
76 PL promoters,, PCRs were performed using F-*ccdB*-SD-OK/R-PU-SD-OK and F-PL-
77 SD-T/R-PL-SD-T primer pairs, respectively. Finally, to generate the pFW plasmid, an
78 operator O1 sequence (see ³⁸) was added into the PL promoter by PCR amplification of
79 the pFW2 plasmid using F-PL-O1/R-PL-O1 primers.

80 To generate the pPW-R6K, pFW-R6K and pNctrl-R6K plasmids we first amplified the
81 R6K replication origin using F-R6K-weapon/R-R6K-weapon primers and the pMP7⁴⁰
82 plasmid as template. Then, the pPW, pFW and pNctrl plasmids were amplified using F-

83 weapon-R6K/R-weapon-R6K primers. Finally, PCR fragments were ligated by Gibson
84 assembly³⁵.

85

86 **Δ toxRS strain construction**

87 DNA regions 500 bp upstream and downstream of the *toxRS* operon were amplified
88 using F-toxRup-p7/R-toxRups and F-toxSdow/R-toxSdow-p7, respectively. The
89 amplified fragments were ligated by Gibson assembly³⁵ and then cloned into an R6K γ -
90 *ori*-based suicide vector, pSW7848⁴⁰ that encodes the *ccdB* toxin gene under the
91 control of an arabinose-inducible promoter, P_{BAD}. For conjugal transfer of plasmids into
92 *V. cholerae* strains, *E. coli* β 3914 was used as the donor. Clones where integration of
93 the entire plasmid in the chromosome by single crossover occurred were selected.
94 Elimination of the plasmid backbone resulting from a second recombination step was
95 selected as described ref 39.

96

97 **Transformation assays**

98 DH5 α chimiocompetent cells (Invitrogen) were transformed with 150 ng of pTox,
99 pToxInt or pN plasmids (Supplementary Fig. 1a). Transformants were then tested in Sp
100 containing media with glucose or arabinose to analyze toxin integrity. 10 to 12% of
101 pTox-transformed clones from were able to grow in the presence of arabinose. Four
102 independent clones were analyzed by sequencing and they all carried an insertion
103 sequence in the *ccdB* toxin gene. These clones were responsible for pTox
104 transformation rate decrease in comparison with the pToxInt and pN plasmids.

105 DH5 α cells (Invitrogen) were co-transformed with two plasmids simultaneously. Both
106 plasmids were then simultaneously selected (Supplementary Fig.4).

107 Transformation of the donor strain β 3914 was performed in the presence of DAP.

108

109 **Growth tests**

110 Eighteen independent clones from DH5 α transformation were inoculated in p96
111 microplates containing LB media with Sp and glucose. The TECAN Infinite 200
112 microplate reader (TECAN, Männedorf, Germany) was used to determine growth
113 curves, with absorbance (620nm) taken at 6-minute intervals for a period of 12 h. The
114 obtained OD values were plotted as seen on Supplementary Fig. 1b.

115 In Supplementary Fig. 2 for analysis of bactericide effect of CcdB toxin: *V. cholerae*
116 O139 was co-transformed with antitoxin-*ccdA* (pBAD24-*ccdA*) and pPW plasmids in
117 the presence of arabinose allowing the antitoxin to be expressed. pPW plasmid
118 contains the toxin-intein under the control of *ompU* promoter, which is always active in
119 *V. cholerae*. Bacteria culture supplemented with antibiotics for maintaining both
120 plasmids and arabinose, were diluted at OD=0.5 (time 0h). Then bacteria were washed
121 three times with MH media with antibiotics and glucose, in order to switch off antitoxin
122 expression, and incubated for 4h at 37°C. Total bacteria were calculated by the CFU/ml
123 at time 0h and 4h present in MH media with antibiotics and with glucose (1%) or
124 arabinose (0,2%). Data numbers were calculated from four independent experiments
125 (n=4).

126

127 **Conjugation assays.**

128 Overnight cultures of donor and recipient strains were diluted 1:100 in culture media
129 with antibiotic and grown at 37°C for 2-3 hours. Then, cultures were diluted to an OD₆₀₀
130 = 0.5. The different conjugation experiments were performed by a filter mating
131 procedure described previously⁴¹ with a donor/recipient ratio of 1::1. When the
132 recipients were composed of a mixed population the donor/mixed-recipient ratio was
133 1::0.5-0.5. Before mixing the different bacteria, cultures were washed three times with
134 fresh media to remove antibiotics. In Supplementary Table 2 bacteria were mixed in
135 different proportions (2:1 and 3:1) to test whether this would impact conjugation
136 efficiency. Conjugation was performed during 4h at 37°C on filter in MH plates

137 supplemented with DAP (and containing NaCl until 332mM final concentration in the
138 case of *V. vulnificus*).

139

140 ***In vivo* conjugation in zebrafish larvae and *Artemia salina***

141 All animal experiments described in the present study were conducted at the Institut
142 Pasteur according to European Union guidelines for handling of laboratory animals
143 (http://ec.europa.eu/environment/chemicals/lab_animals/home_en.htm) and were
144 approved by the Institut Pasteur Animal Care and Use Committee and the Direction
145 Sanitaire et Veterinaire de Paris under permit #A-75-1061. Conjugative killing was
146 assessed as follow. Four-day-postfertilization zebrafish larvae were exposed to water
147 containing 10^4 CFU/ml of *V. cholerae* O139 for 2 hours at 27°C (Figure 4a) or a 1::1
148 mixed population containing 10^5 CFU/ml *V. cholerae* O139 + *V. cholerae* O1 (Figure
149 5a, mix *Vibrio*) for 2 hours at 27°C. Then, larvae were washed in sterile water three
150 times and then placed into a well containing 10^7 or 10^6 CFU/ml (Figure 4a, *V. cholerae*
151 O139 and mix *Vibrio*, respectively) of the *E. coli* β 3914- Δ dap donor strain containing
152 either the pN_{ctrl} or pFW plasmid for 24 hours at 27°C. In Supplementary Fig. 11b and
153 11c, infection dose for *Vibrio* was the same than for Fig. 4a. Larvae were transferred to
154 bacteria-free wells, washed in sterile water three times and then placed into a well
155 containing Tricaine (Sigma-Aldrich #E10521) at 200 mg/ml to euthanize them. Finally,
156 they were transferred to a tube containing calibrated glass beads (acid washed, 425
157 μ m to 600 μ m, Sigma-Aldrich #G8722) and 500 μ l of water. Five larvae were mashed
158 using FastPrep® Cell Disrupter (BIO101/FP120 QBioGene) for 45 seconds at
159 maximum speed (6,5 m/sec) to analyze their microbiota (Supplementary Fig. 11) in MH
160 Media + X-gal or TCBS media for selection of *V. cholerae*. Blue bacteria corresponding
161 to *V. cholerae* O139 were detected in MH media. Transconjugants selection was done
162 into MH Media + X-gal and Sp and then, replication of these MH plates were done on
163 TCBS media to specific identify *V. cholerae*. Strain identity was confirmed through

164 yellow color development in TCBS *Vibrio* specific media. The amoeba *Tetrahymena*
165 *thermophila* (*T. thermophila*) was added to feed larvae during the experiment.

166

167 Groups of 225±15 larvae of *Artemia salina* stage nauplii suspended in 1ml volume of
168 seawater were washed using sterile cell strainer Nylon filters 100 µm pore size
169 (Falcon) and three times with the same volume (3x1ml) of sterile PBS (D8537, Sigma).
170 Nauplii were suspended in 1ml PBS and then infected with 10⁷ *V. cholerae* O1 or a mix
171 of 10⁷ *V. cholerae* O1 and O139 for 2 hours in agitation at 27°C. Then nauplii were
172 washed as previously described and exposed to 10⁷ of β3914 -Δ*dap* bacteria with
173 pN_{ctrl} or pFW plasmid for 4 hours at 27°C. These experiments were repeated four times
174 independently. The microbiota from 1ml containing 225±15 nauplii were analyzed as
175 previously described for zebrafish. In the case of *Artemia*, we have used M63B1
176 minimal media where *Artemia* feel asleep and then put them on ice, previous the use of
177 fast-prep (FastPrep® Cell Disrupter (BIO101/FP120 QBioGene) for 45 seconds at
178 maximum speed (6,5 m/sec)). Transconjugants were selected from 225±15 nauplii
179 after pN_{ctrl} or pFW conjugation treatment into MH media with Sp and X-gal
180 (Supplementary Fig. 12a,b). For the identification of *V. cholerae* in the mix of both
181 serogroups (Fig. 4b and Supplementary Fig. 12b), replication of these MH plates were
182 done into TCBS media to specifically identify *V. cholerae*. Strain identity was confirmed
183 through yellow color development in TCBS *Vibrio* specific media.

184

185 **Co-localization of *E. coli* and *V. cholerae* in the zebrafish larvae and *A. salina* by**
186 **Microscopy.**

187 Co-localization of *E. coli* and *V. cholerae* in the zebrafish larvae was assessed as
188 follow. Four-day-postfertilization zebrafish larvae were exposed to water containing 10⁶
189 CFU/ml *V. cholerae* O1-GFP for 2 hours at 27°C. Then washed in sterile water three
190 times and then placed into a well containing 10⁷ CFU/ml of *E. coli*-RFP for 24 hours at
191 27°C. Larvae were removed from the well and then placed into a well containing

192 Tricaine for euthanize them. Infected and non-infected larvae were visualized by
193 fluorescence microscopy (EVOS FL microscope-Life technologies) using appropriate
194 wavelength conditions enabling or not the visualization of GFP and RFP. Fluorescence
195 was only detected in infected larvae and more precisely into the gut where both
196 bacteria are co-localized.

197 In the case of *A. salina* stage nauplii the microscopy experiment was done using 10^7 *V.*
198 *cholerae*-GFP for 2 hours in agitation at 27°C. Then nauplii were washed as previously
199 described and exposed to 10^7 of *E. coli*-RFP strain for 2 hours. Microscopy conditions
200 were performed as for zebrafish experiment.

201

202 **Statistics**

203 In Supplementary Fig. 9, one-way ANOVA with Dunnett's Multiple Comparison Test
204 was performed. PNcontrol-R6K vs pPW-R6K, Mean Diff. = 2.383e+008, q = 4.183,
205 **P<0.05, 95% CI of diff = (8.937e+007 to 3.871e+008). PNcontrol-R6K vs pFW-R6K,
206 Mean Diff. = 2.308e+008, q = 4.227, **P<0.05, 95% CI of diff = (9.187e+007 to
207 3.896e+008).

208 In Supplementary Fig. 13, one-sided t-test Mann Withney was performed. *E. coli* SXT
209 vs *E. coli* MG1655. P value = 0.0143. *P < 0.05.

210

211 **References**

212

- 213 35. Gibson, D. G. *et al.* Enzymatic assembly of DNA molecules up to several
214 hundred kilobases. *Nat. Methods* **6**, 343–345 (2009).
- 215 36. Guzman, L. M., Belin, D., Carson, M. J. & Beckwith, J. Tight regulation,
216 modulation, and high-level expression by vectors containing the arabinose
217 P(BAD) promoter. *J. Bacteriol.* **177**, 4121–4130 (1995).
- 218 37. Bartolomé, B., Jubete, Y., Martínez, E. & de la Cruz, F. Construction and
219 properties of a family of pACYC184-derived cloning vectors compatible with

- 220 pBR322 and its derivatives. *Gene* **102**, 75–78 (1991).
- 221 38. Poulin-Laprade, D. & Burrus, V. A γ Cro-like repressor is essential for the
222 induction of conjugative transfer of SXT/R391 elements in response to DNA
223 damage. *J. Bacteriol.* **197**, 3822–3833 (2015).
- 224 39. Demarre, G. *et al.* A new family of mobilizable suicide plasmids based on broad
225 host range R388 plasmid (IncW) and RP4 plasmid (IncP α) conjugative
226 machineries and their cognate *Escherichia coli* host strains. *Res. Microbiol.* **156**,
227 245–255 (2005).
- 228 40. Val, M. E., Skovgaard, O., Ducos-Galand, M., Bland, M. J. & Mazel, D. Genome
229 engineering in *Vibrio cholerae*: A feasible approach to address biological issues.
230 *PLoS Genet.* **8**, (2012).
- 231 41. Biskri, L., Bouvier, M., Guérout, A., Boissard, S. & Mazel, D. Comparative study
232 of class 1 integron and *Vibrio cholerae* superintegron integrase activities. *J*
233 *Bacteriol* **187**, 1740–1750 (2005).
- 234

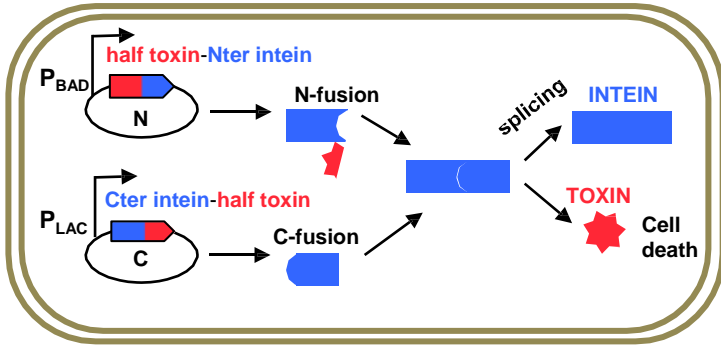
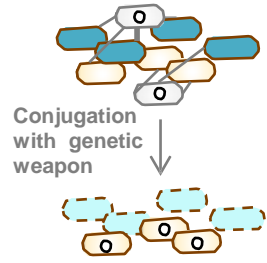
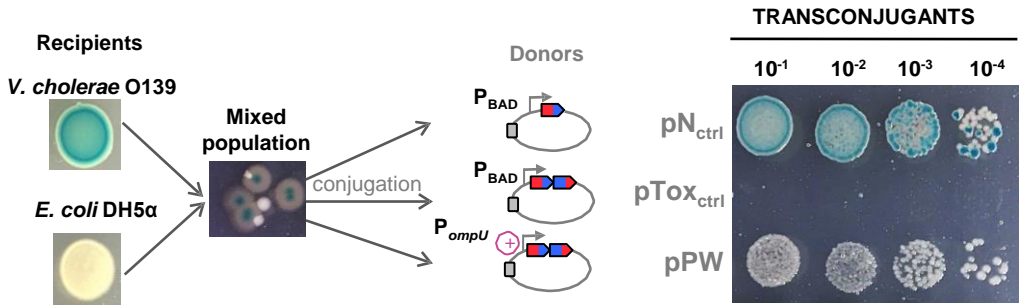
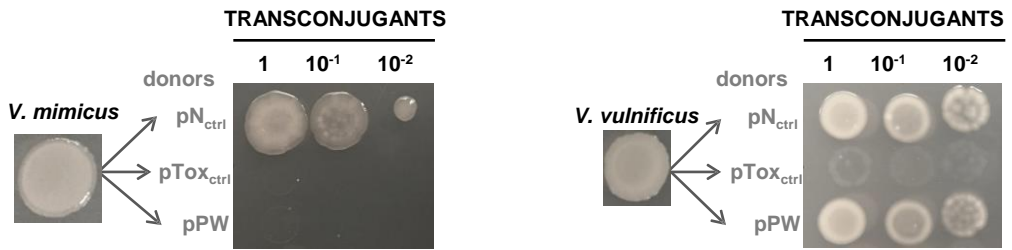
a**b****c****d**

Figure 1

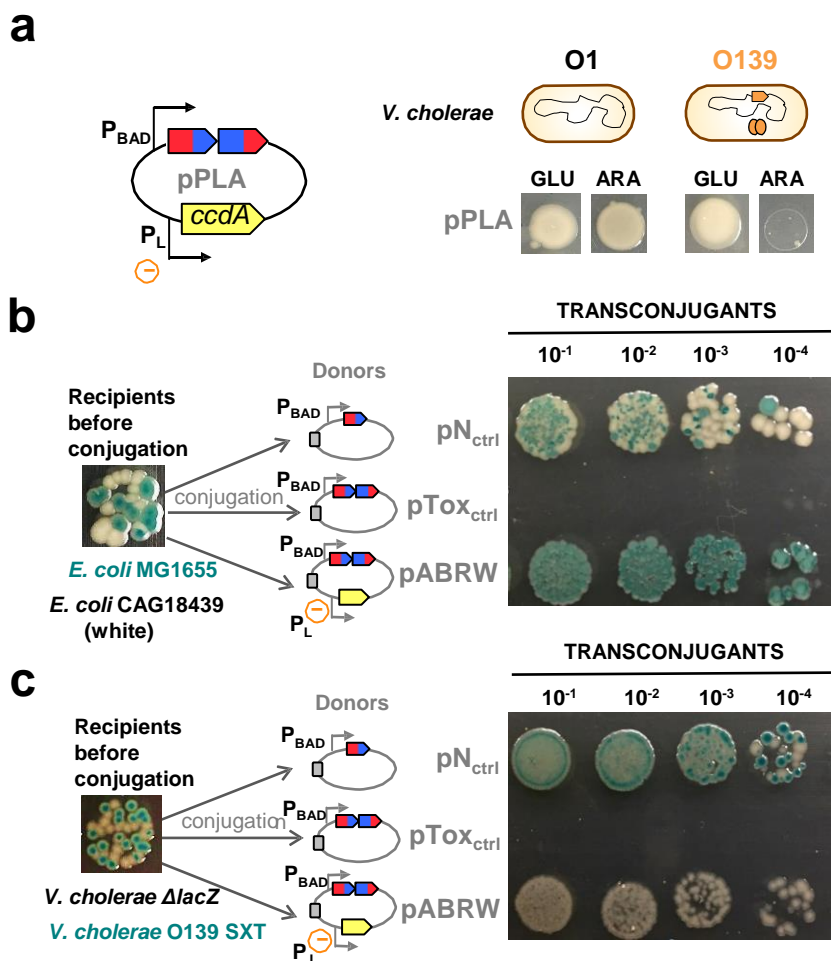


Figure 2

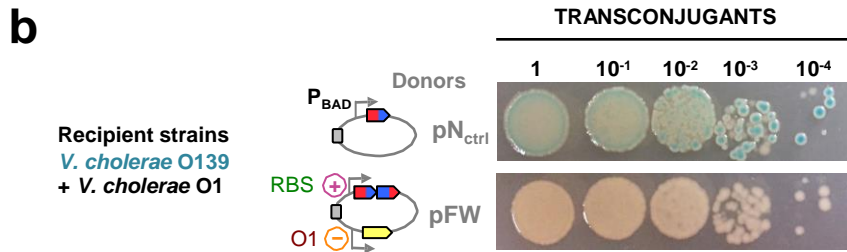
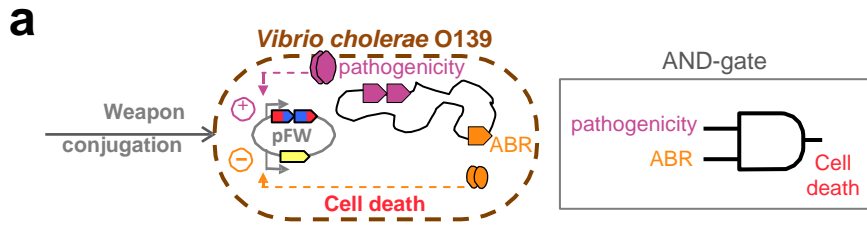


Figure 3

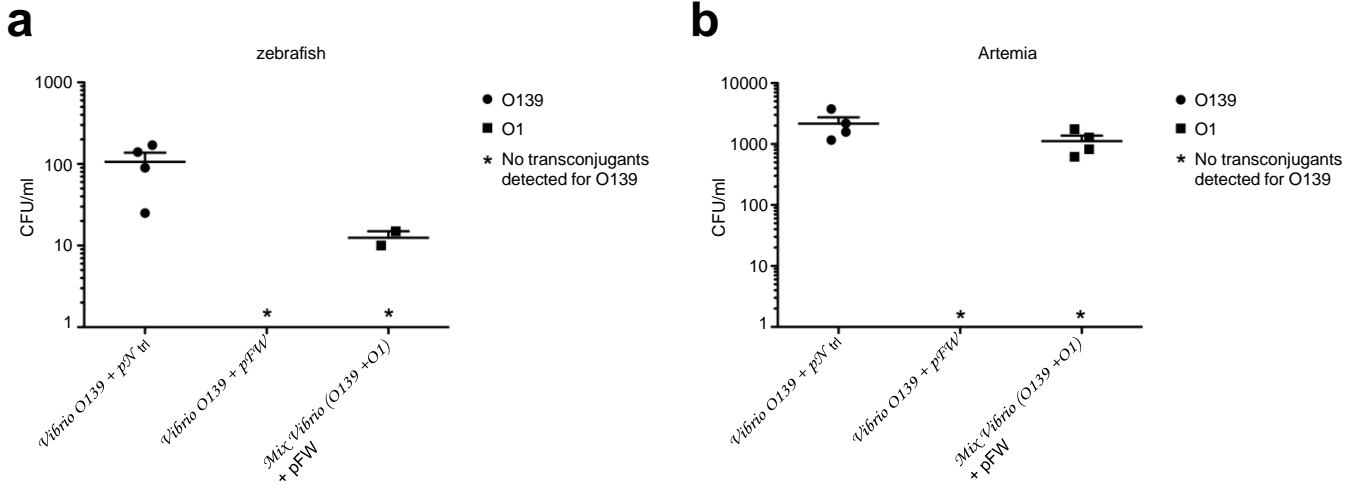


Figure 4